Electronic Supplementary Material (ESI) for Catalysis Science & Technology.

Supporting Information

For

Mechanistic studies on catalytic alkane oxidation by the Murahashi's aldehyde/O_2/copper(II) system

---

*Kohei Yamaguchi, Yuya Uemura, Hideki Sugimoto, Rin Ito, Yuma Morimoto and Shinobu Itoh **

Department of Molecular Chemistry, Division of Applied Chemistry, Graduate School of Engineering, Osaka University, 2-1 Yamadaoka, Suita, Osaka 565-0871, Japan.

Contents

Table S1. Oxidation of cyclohexane by O_2/**1**/ PhCHO system in the different solvent systems.

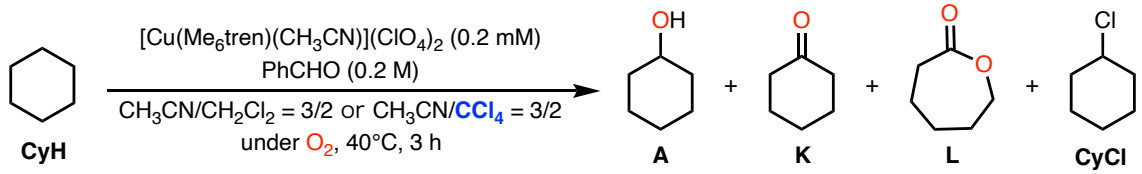

Solvent	Yield/mM[a] (%) [b]			
	A	**K**	**L**	**CyCl**
CH_3CN/CH_2Cl_2	11 (51%)	9.5 (44%)	0.4 (1%)	0.6 (3%)
CH_3CN/CCl_4	5.0 (43%)	4.2 (37%)	0.3 (3%)	2.0 (**17**%)

Reaction conditions: [**1**] = 0.2 mM, [PhCHO] = 0.2 M, [CyH] = 2.0 M at 40ºC under O_2. [a] The amount of the products are determined by GC-FID using calibration curves of the products. [b] Products ratio (%) = 100×[X]/[P] (P = **A** + **K** + **L** + **CyCl**, X = **A**, **K**, **L** or **CyCl**).

Table S2. Comparison of product distribution pattern before and after quenching the reaction with PPh_3.

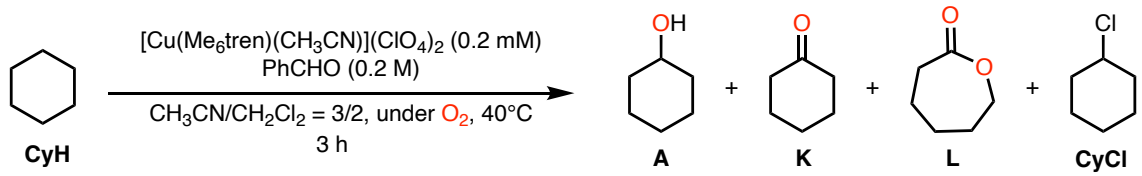

Quencher	Yield/mM[a] (%)[b]			
	A	**K**	**L**	**Cy^{6}Cl**
–	11(51%)	9.5 (44%)	0.4 (1%)	0.6 (3%)
PPh_3	12 (54%)	9.1 (41%)	0.3 (2%)	0.7 (3%)

Reaction conditions: [**1**] = 0.2 mM, [PhCHO] = 0.2 M, [CyH] = 2.0 M in CH_3CN/CH_2Cl_2 (*v*/*v* = 3/2) at 40ºC for 3 h under O_2. [a] The amount of the products are determined by GC-FID using calibration curves of the products. [b] Product ratio (%) = 100×[X]/[P] (P = **A** + **K** + **L** + **CyCl**, X = **A**, **K**, **L** or **CyCl**)

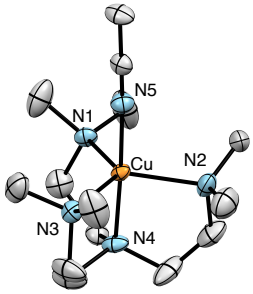

1 ([Cu(Me$_6$tren)(CH$_3$CN)](ClO$_4$)$_2$)

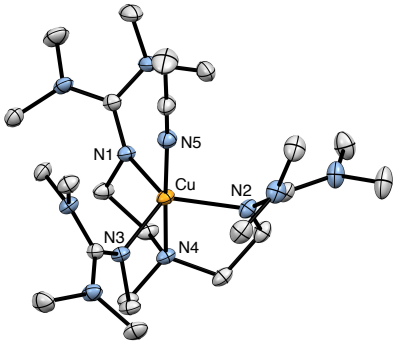

2 ([Cu(TMG$_3$tren)(CH$_3$CN)](BPh$_4$)$_2$)

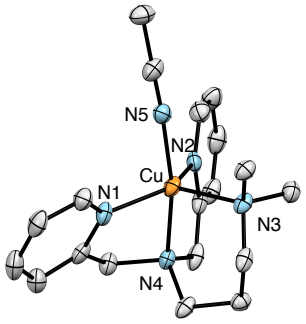

3 ([Cu(Me$_2$-pp3)(CH$_3$CN)](ClO$_4$)$_2$)

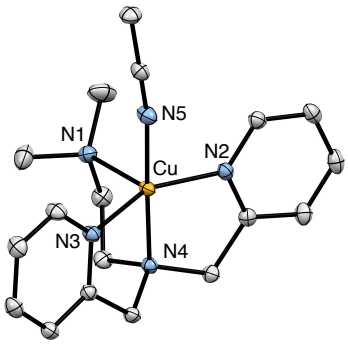

4 ([Cu(Me$_2$-uns-penp)(CH$_3$CN)](ClO$_4$)$_2$)

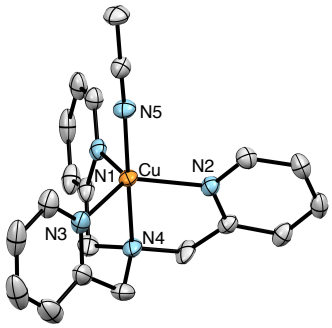

5 ([Cu(TPA)(CH$_3$CN)](ClO$_4$)$_2$)

Fig. S1 ORTEP drawings of Cu^{II}-complexes **1**–**5** showing 50% probability thermal-ellipsoids. Hydrogen atoms and counter cations are omitted for clarity.

Table S3. Summary of the X-ray crystallographic data of **1** and **2**.

Compound	**1** $[Cu(Me_6tren)(CH_3CN)](ClO_4)_2$	**2** $[Cu(TMG_3tren)(CH_3CN)](BPh_4)_2$
Empirical formula	$C_{14}H_{33}N_5CuCl_2O_8$	$C_{71}H_{91}B_2CuN_{11}$
Formula weight	533.89	1183.70
Temperature/K	296	115
Crystal system	monoclinic	triclinic
Space group	$P2_1/n$	P-1
a/Å	9.7458(9)	12.9525(9)
b/Å	15.2404(14)	13.3361(11)
c/Å	15.8334(14)	20.9485(14)
α/°	90	83.572(6)
β/°	91.303(6)	78.793(5)
γ/°	90	66.559(5)
Volume/Å^3	2351.1(4)	3254.2(4)
Z	4	2
ρ_{calc}g/cm^3	1.392	1.208
μ/mm^{-1}	1.196	0.386
F(000)	1028	1266
Crystal size/mm^3	0.1 × 0.1 × 0.1	0.1 × 0.1 × 0.1
Radiation	MoKα (λ = 0.71075)	MoKα (λ = 0.71075)
2Θ range for data collection/°	3.71 to 54.964	3.474 to 54.97
Index ranges	$-12 \le h \le 12$, $-19 \le k \le 19$, $-18 \le l \le 20$	$-16 \le h \le 16$, $-17 \le k \le 17$, $-23 \le l \le 27$
Reflections collected	22294	32124
Independent reflections	5393 [R_{int} = 0.0305, R_{sigma} = 0.0258]	14856 [R_{int} = 0.0254, R_{sigma} = 0.0358]
Data/restraints/parameters	5393/0/287	14856/0/779
Goodness-of-fit on F^2	0.985	1.088
Final R indexes [I>=2σ (I)]	R_1 = 0.0740, wR_2 = 0.2078	R_1 = 0.0404, wR_2 = 0.0986
Final R indexes [all data]	R_1 = 0.0861, wR_2 = 0.2204	R_1 = 0.0582, wR_2 = 0.1127
Largest diff. peak/hole / e Å^{-3}	2.04/-1.32	0.39/-0.53

[a] $R = \sum||F_o| - |F_c||/\sum|F_o|$. [b] $R_w = [\sum(w(|F_o| - |F_c|)^2/\sum wF_o^2)]^{1/2}$

Table S4. Summary of the X-ray crystallographic data of **3** and **4**.

Compound	**3** $[Cu(Me_2\text{-}pp3)(CH_3CN)](ClO_4)_2$	**4** $[Cu(Me_2\text{-}unspenp)(CH_3CN)](ClO_4)_2$
Empirical formula	$C_{19}H_{27}N_5CuCl_2O_8$	$C_{18}H_{25}N_5CuCl_2O_8$
Formula weight	587.89	573.87
Temperature/K	115	115
Crystal system	monoclinic	monoclinic
Space group	$P2_1/c$	C2/c
a/Å	11.4909(12)	20.0899(17)
b/Å	9.9244(12)	10.2143(10)
c/Å	21.336(2)	23.1418(18)
α/°	90	90
β/°	99.433(7)	101.316(7)
γ/°	90	90
Volume/Å^3	2400.2(5)	4656.5(7)
Z	4	8
ρ_{calc}g/cm^3	1.627	1.637
μ/mm^{-1}	1.188	1.223
F(000)	1212	2360
Crystal size/mm^3	0.1 × 0.1 × 0.1	0.1 × 0.1 × 0.1
Radiation	MoKα (λ = 0.71075)	MoKα (λ = 0.71075)
2Θ range for data collection/°	3.594 to 54.972	3.59 to 54.964
Index ranges	$-14 \le h \le 14$, $-12 \le k \le 12$, $-27 \le l \le 24$	$-26 \le h \le 25$, $-13 \le k \le 13$, $-30 \le l \le 29$
Reflections collected	21337	22050
Independent reflections	5492 [R_{int} = 0.0714, R_{sigma} = 0.0648]	5333 [R_{int} = 0.0134, R_{sigma} = 0.0121]
Data/restraints/parameters	5492/0/319	5333/0/315
Goodness-of-fit on F^2	1.092	1.084
Final R indexes [I>=2σ (I)]	R_1 = 0.1017, wR_2 = 0.2503	R_1 = 0.0289, wR_2 = 0.0792
Final R indexes [all data]	R_1 = 0.1222, wR_2 = 0.2656	R_1 = 0.0312, wR_2 = 0.0830
Largest diff. peak/hole / e Å^{-3}	1.77/-1.70	0.71/-1.01

[a] $R = \sum||F_o| - |F_c||/\sum|F_o|$. [b] $R_w = [\sum(w(|F_o| - |F_c|)^2/\sum wF_o^2)]^{1/2}$

Table S5. Summary of the X-ray crystallographic data of **5**.

Compound	**5** [Cu(TPA)(CH_3CN)](ClO_4)$_2$
Empirical formula	$C_{20}H_{21}N_5CuCl_2O_8$
Formula weight	593.86
Temperature/K	115
Crystal system	monoclinic
Space group	$P2_1$
a/Å	10.2096(11)
b/Å	9.5739(10)
c/Å	12.8306(11)
α/°	90
β/°	106.747(7)
γ/°	90
Volume/Å^3	1200.9(2)
Z	2
ρ_{calc}g/cm^3	1.050
μ/mm^{-1}	0.971
F(000)	391
Crystal size/mm^3	0.1 × 0.1 × 0.1
Radiation	MoKα (λ = 0.71075)
2Θ range for data collection/°	5.394 to 54.964
Index ranges	-13 ≤ h ≤ 13, -12 ≤ k ≤ 12, -15 ≤ l ≤ 16
Reflections collected	11450
Independent reflections	5272 [R_{int} = 0.0262, R_{sigma} = 0.0389]
Data/restraints/parameters	5272/1/326
Goodness-of-fit on F^2	1.040
Final R indexes [I>=2σ (I)]	R_1 = 0.0369, wR_2 = 0.0895
Final R indexes [all data]	R_1 = 0.0421, wR_2 = 0.0918
Largest diff. peak/hole / e Å^{-3}	0.61/-0.46

[a] $R = \sum||F_o| - |F_c||/\sum|F_o|$. [b] $R_w = [\sum(w(|F_o| - |F_c|)^2/\sum wF_o^2)]^{1/2}$

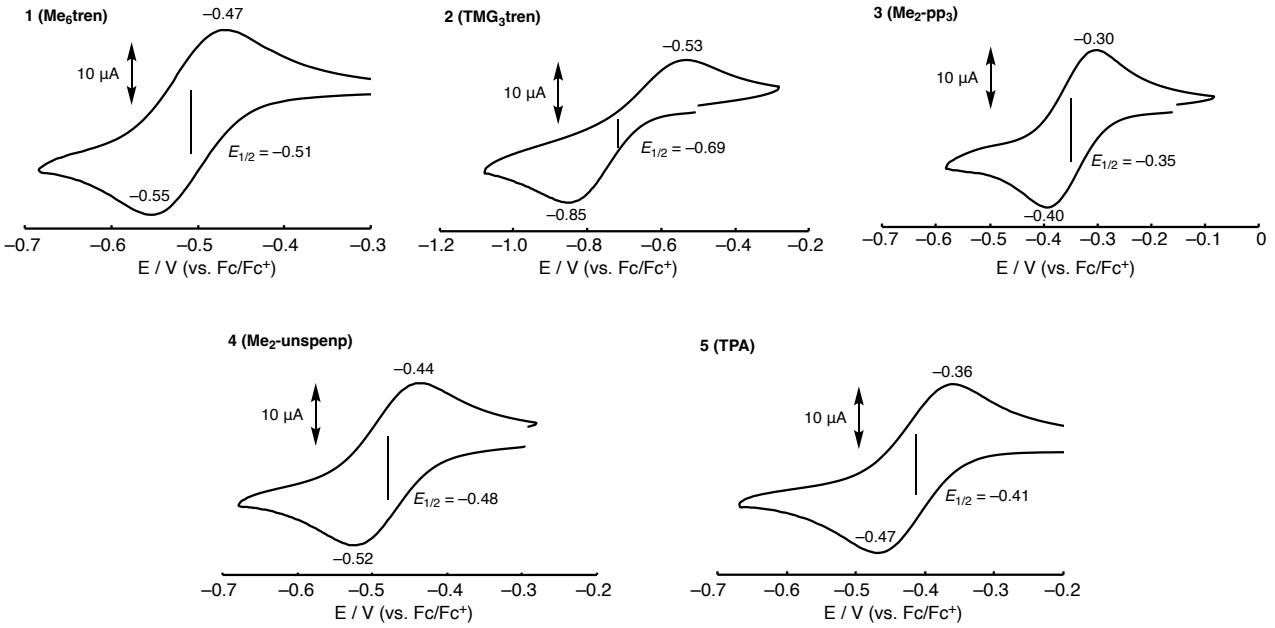

Fig. S2 Cyclic voltammograms of Cu^{II}-complexes (1.0 mM) in CH_3CN containing $TBAPF_6$ (0.1 M). WE: glassy carbon (GC), CE: Pt wire, PE: Ag/Ag^+. Sweep rate: 100 mV/s, Solvent: CH_3CN.

Table S6. Acyl radical trapping experiment using CCl_4.

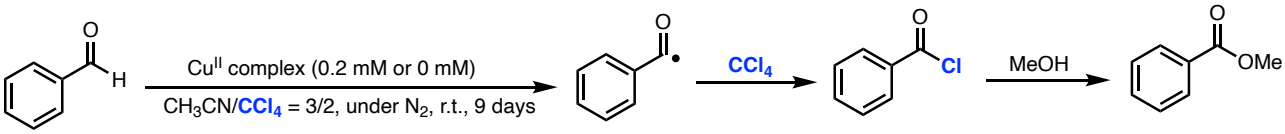

Complex	Redox potential/V[b]	Yield of PhC(O)OMe/mM[a]
1	–0.51	4.1
[Cu(TEPA)OTf](OTf)	+0.05	4.2
None	–	4.8

Reaction conditions: [Cu^{II}-complex] = 0.2 mM, [PhCHO] = 0.2 M, at room temperature for 9 days under anaerobic conditions. [a] The amounts of the products are determined by GC-FID using calibration curves of the products. [b] In acetonitrile vs. Fc/Fc^+.

Acyl radical trapping experiment using acrylonitrile

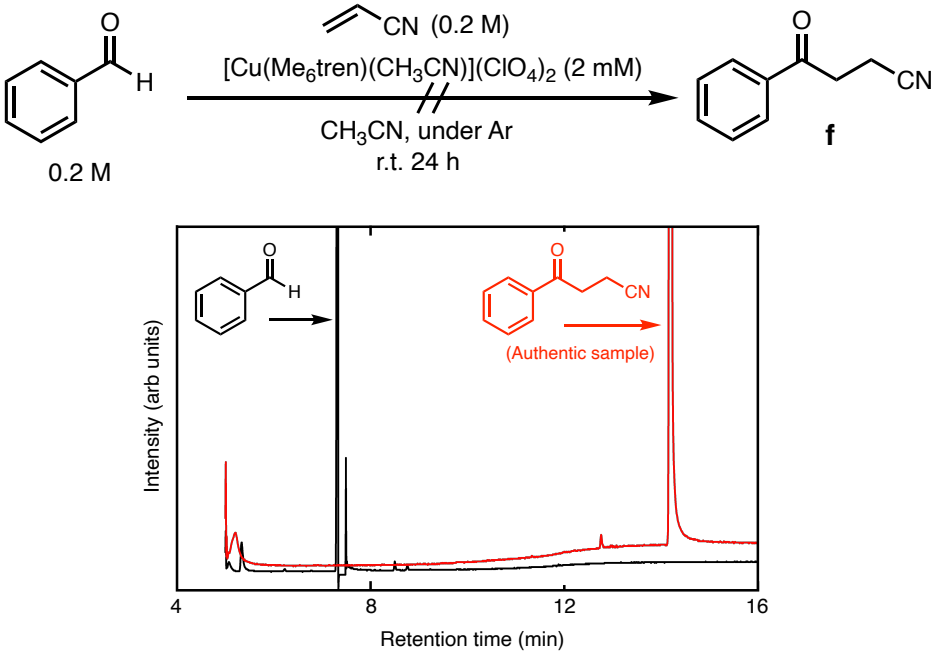

Fig. S3 GC-MS charts of the reaction mixture (black) and the authentic sample (red).

Procedure. PhCHO (100 eq.) and acrylonitrile (100 eq.) were added to an acetonitrile solution (1 mL) of **1** (2 mM). The reaction mixture was stirred for 24 h at room temperature under Ar. After quenching the reaction by passing the reaction mixture through an alumina-column, products were analyzed by GC-MS (Fig. S3).

Discussion. If acyl radical **a** was formed, it might be trapped by acrylonitrile to generate radical intermediate **e** (Scheme S4). Although the BDE of **e** (PhC(O)CH$_2$**CH$_2$**CN) is not known, it is expected to have a value similar to that of propionitrile (CH$_3$**CH$_2$**CN: 94.0 ± 3.0 kcal mol^{-1}). Therefore, the radical intermediate **e** may abstract hydrogen atom from benzaldehyde (PhC(O)–H: 88.7 ± 2.6 kcal mol^{-1} uo, Y.-R. (**2007**). Comprehensive Handbook of Chemical Bond Energies (1st ed.). CRC Press.) to give product **f** and regenerate **e**, making a chain reaction. However, no product **f** was identified at all, suggesting that the effect of aldehyde activation by Cu^{II} is negligible.

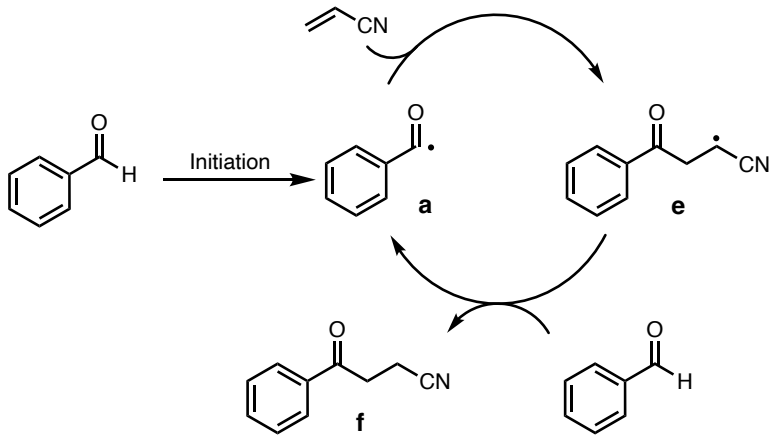

Acyl radical Trapping Experiment Using TEMPO

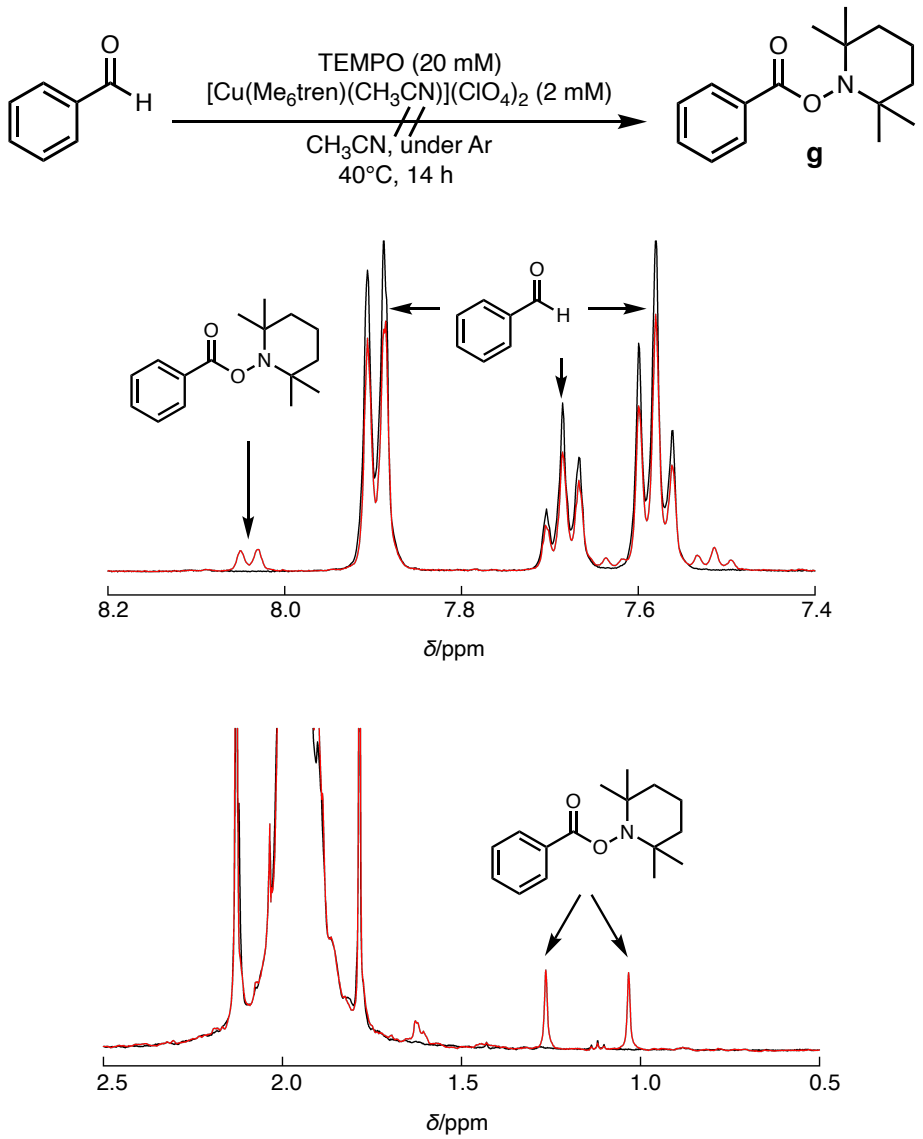

Fig. S4 ^{1}H-NMR spectra of the reaction mixture (black) and authentic sample of TEMPO-adduct **g** (red) in CD_3CN.

Procedure. PhCHO (100 eq.) and TEMPO (10 eq.) were added to an acetonitrile solution (3 mL) of **1** (2 mM). The reaction mixture was stirred for 14 h at 40℃ under Ar. After quenching the reaction by passing the reaction mixture through an alumina-column, products were analyzed by ^{1}H-NMR. TEMPO-additive was synthesized according to the reported procedure.

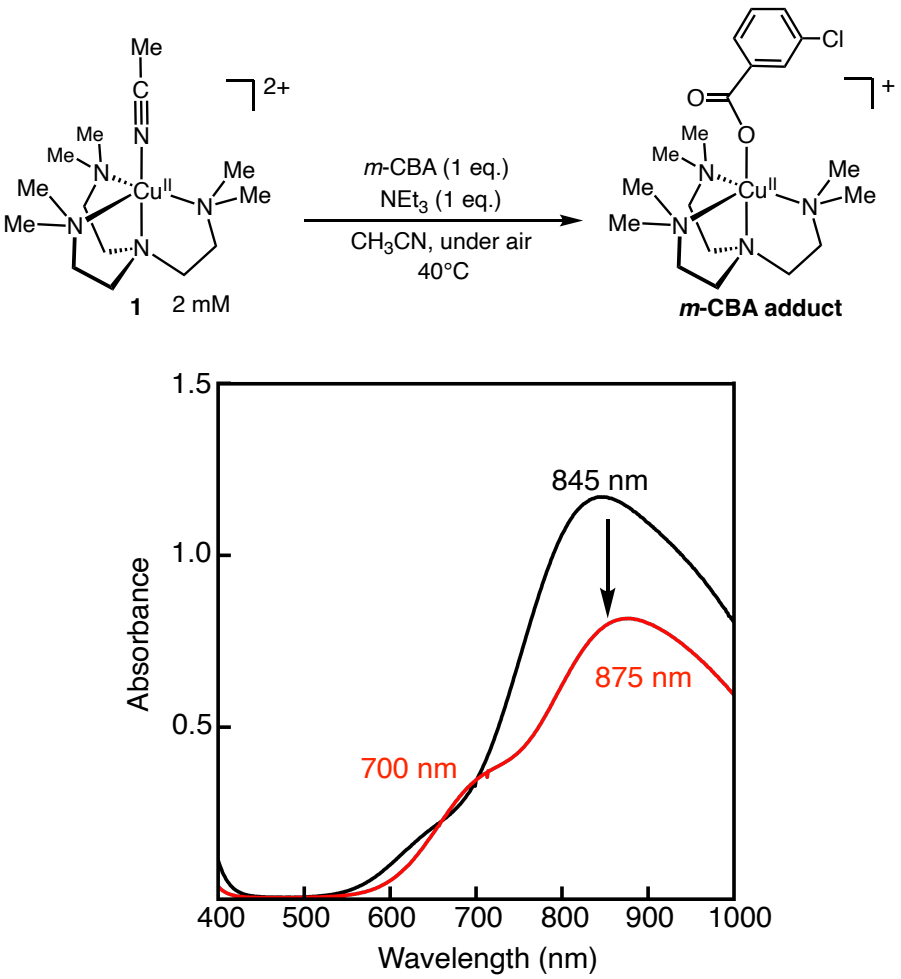

Fig. S5 UV-vis spectral change observed in the reaction of **1** (2 mM) with 1 equiv of *m*-CBA in the presence of triethylamine (1 equiv) in CH_3CN at 40°C.

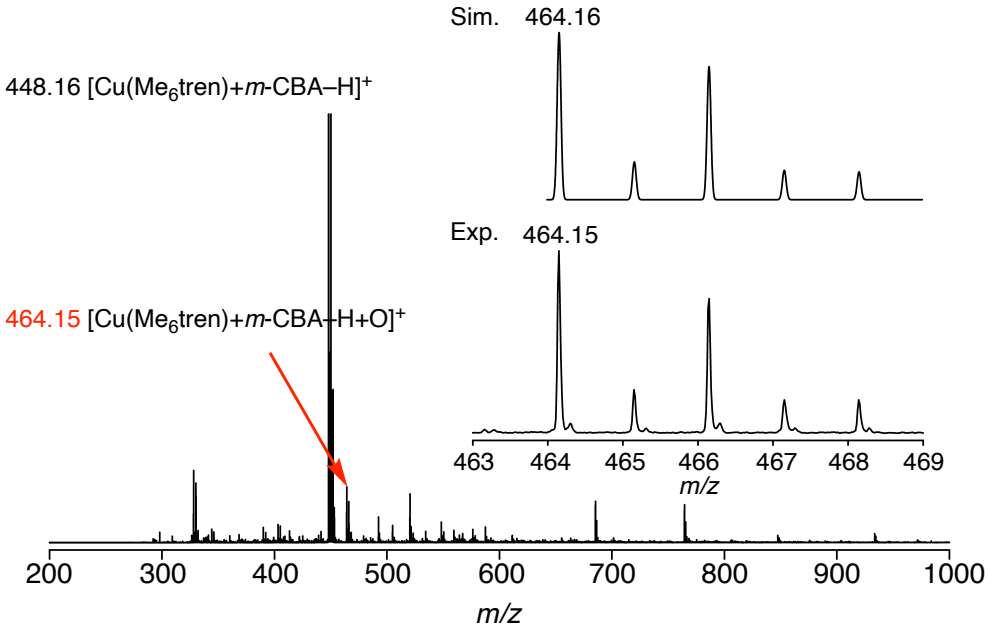

Fig. S6 ESI-MS spectrum of the reaction mixture of **1** and *m*-CPBA (10 equiv) in acetonitrile. Inset: Expanded spectrum and its simulation spectrum. Reaction conditions: [**1**] = 2 mM, [*m*-CPBA] = 20 mM at 40 ºC under air. The peaks for the *m*-CBA adduct complex at 448.18 may be generated in the mass measurement.

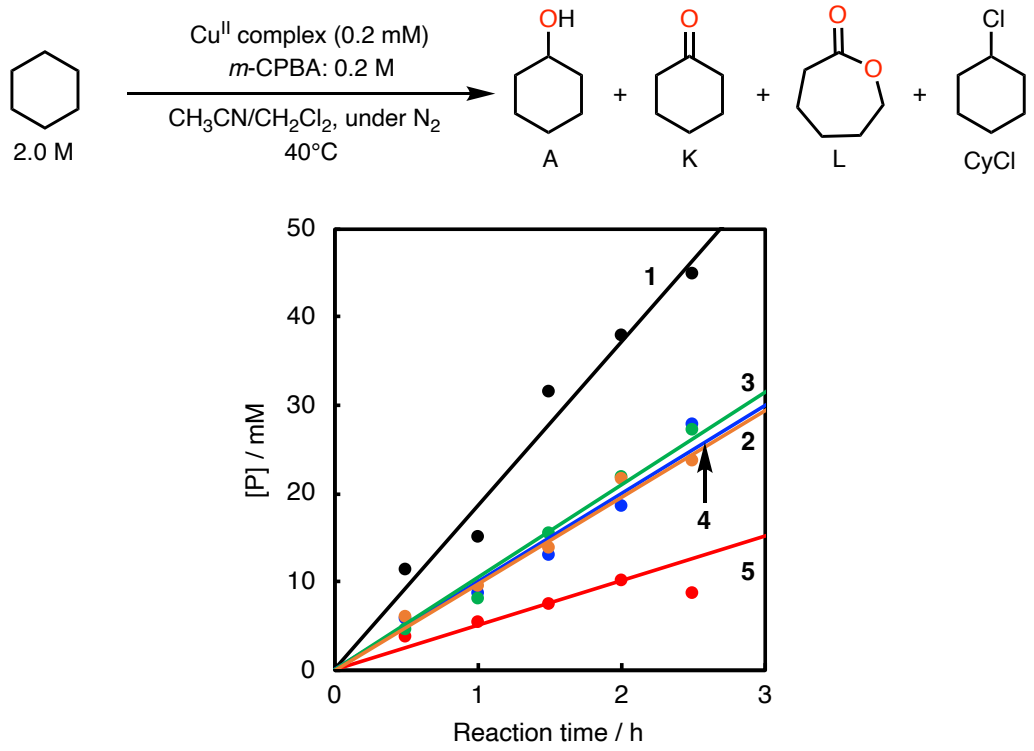

Fig. S7. Oxidation of cyclohexane by *m*-CPBA in the presence of a catalytic amount of Cu^{II}-complex under N_2 atmosphere. Reaction conditions: [Cu^{II}-complex] = 0.2 mM, [*m*-CPBA] = 0.2 M, [Cyclohexane] = 2.0 M at 40 ºC under N_2. [P] = **A** + 2**K** +2**L** + **CyCl**. The time-dependent yields of each product (A, K, L, and CyCl) are presented in the following tables.

[$Cu(Me_6tren)(CH_3CN)](ClO_4)_2$ (**1**)

Time/h	Yield/mM[a]			
	A	**K**	**L**	**Cy^{6}Cl**
0.5	5.7	2.0	0.41	0.82
1.0	7.5	2.6	0.62	1.1
1.5	21	2.7	1.5	2.0
2.0	26	2.9	2.0	2.3
2.5	29	4.1	2.5	2.7

[$Cu(TMG_3tren)(CH_3CN)](BPh_4)_2$ (**2**)

Time/h	Yield/mM[a]			
	A	**K**	**L**	**Cy^{6}Cl**
0.5	3.8	0.72	0	0.73
1.0	4.5	1.3	0.36	1.5
1.5	7.6	1.5	0.75	1.6
2.0	13	2.3	1.2	2.2
2.5	13	2.6	1.3	2.5

[Cu(pro)(CH_3CN)](ClO_4)$_2$ (**3**)

Time/h	Yield/mM[a]			
	A	**K**	**L**	**Cy^{6}Cl**
0.5	2.9	0.75	0	0
1.0	5.7	1.2	0	0
1.5	10	2.1	0.38	0.36
2.0	14	2.7	0.67	0.57
2.5	19	2.6	1.2	0.74

[Cu(Me_2-unspenp)(CH_3CN)](ClO_4)$_2$ (**4**)

Time/h	Yield/mM[a]			
	A	**K**	**L**	**Cy^{6}Cl**
0.5	2.6	1.5	0	0
1.0	4.2	2.2	0	0
1.5	7.3	2.7	0	0.23
2.0	9.9	3.3	0.85	0.35
2.5	15	5.0	1.2	0.56

[Cu(TPA)(CH_3CN)](ClO_4)$_2$ (**5**)

Time/h	Yield/mM[a]			
	A	**K**	**L**	**Cy^{6}Cl**
0.5	1.9	0.84	0	0
1.0	2.8	1.2	0	0
1.5	3.9	1.8	0	0
2.0	5.7	2.1	0	0
2.5	5.1	1.7	0	0

Reaction conditions: [Cu^{II}] = 0.2 mM, [*m*-CPBA] = 0.2 M, [Cyclohexane] = 2.0 M at 40 ºC under N_2.
[a]The amounts of the products are determined by GC-FID using calibration curves of the products.

Titration of perbenzoic acid generated in aerobic oxidation of benzaldehyde.

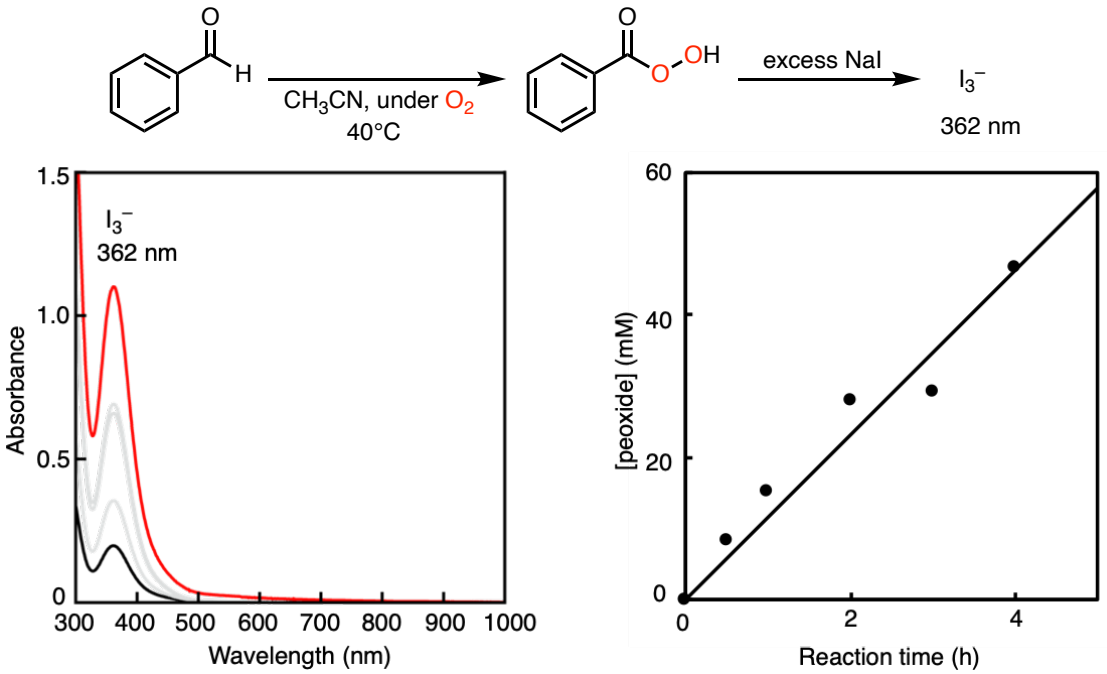

Fig. S8. Spectroscopic titration of perbenzoic acid by NaI (left) and a time dependent formation perbenzoic acid. Reaction conditions: [PhCHO] = 0.2 M, in CH_3CN, at 40℃, under O_2.

Procedure. To minimize the influence of metal particles, aqua regalis rinsed vials and stirrer bars were employed. PhCHO (0.2 M) was added to acetonitrile (1 mL). After stirring for a certain time, the reaction solution was diluted to 1000-fold, added to 2 mL of acetonitrile solution of sodium iodide (0.1 M), and the UV-vis spectrum was measured. The concentration of peroxide species in the reaction solution was determined by the Lambert-Beer law. The molar absorption coefficient for I_3^- (362 nm) in acetonitrile was the reported value.[14]

Oxidation of methane

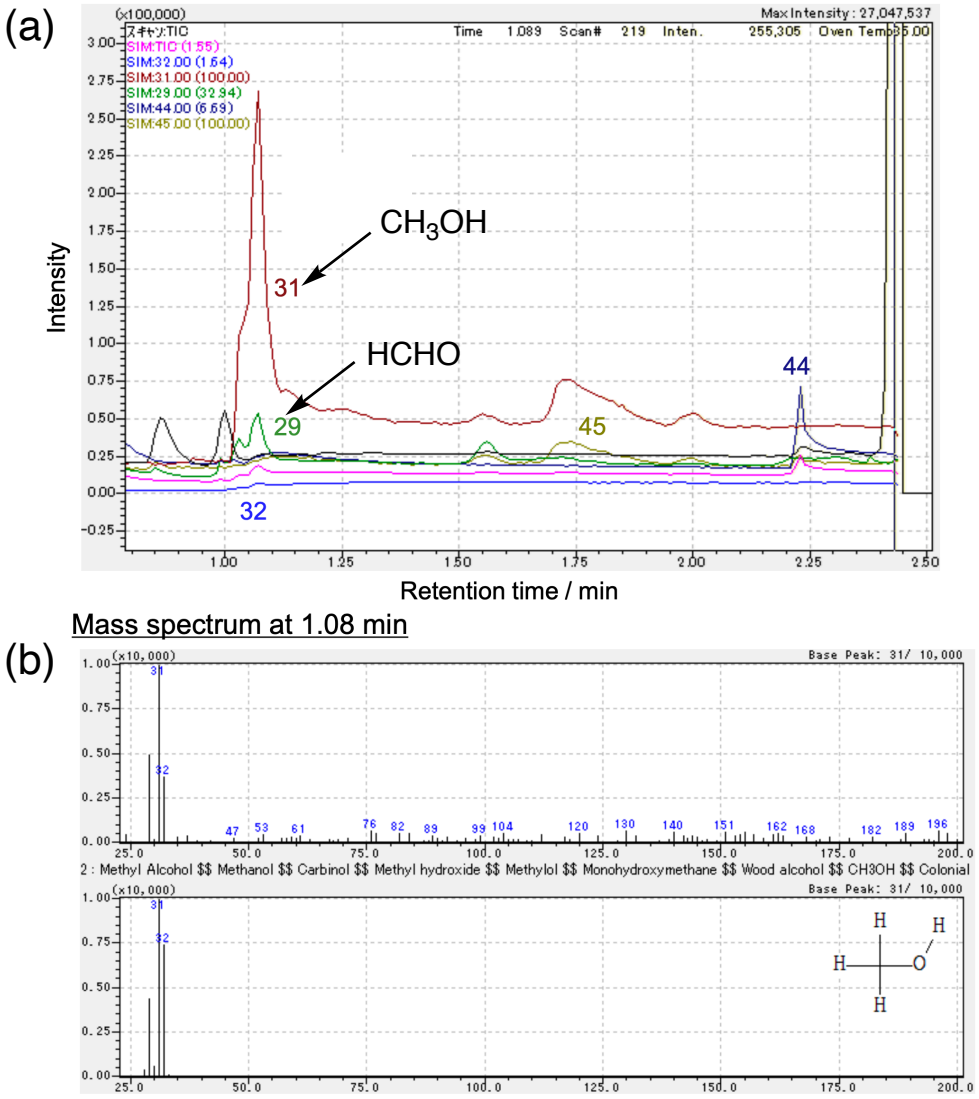

Fig. S9 (a) GC-MS charts of the final reaction solution of the methane oxidation. Selected ion monitoring: *m/z* = 31 for CH_3OH, *m/z* = 29 for HCHO. (b) Mass spectrum at 1.08 min (above) and its simulation spectrum (below).